Clay Minerals (1998) **33**, 349–362

Characteristics and origin of sepiolite (Meerschaum) from Central Somalia

A. SINGER, K. STAHR AND M. ZAREI*

Seagram Center for Soil and Water Sciences, The Hebrew University of Jerusalem, PO Box 12, Rehovot 76100, Israel, and Institut für Bodenkunde u. Standortslehre, Universitat Hohenheim, D-70599 Stuttgart, Germany

(*Received 16 December 1996; revised 3 June 1997*)

ABSTRACT: Nearly pure sepiolite clay crops out in a playa-like depression near El Bur, Central Plateau region of Somalia. The deposit is associated with the Lower to Mid-Eocene Taleh Formation that includes, besides limestone, dolomite and gypsiferous marls, extensive anhydrite and various evaporites, primarily gypsum. The material was examined by XRD, DTA, IR and EM. The XRD and DTA analyses indicated that from 40 cm down to a depth of 300 cm, the material consists of well-crystallized sepiolite, accompanied in some layers by minor calcite and traces of quartz and halite. The chemical composition, determined by XRF, indicated a low-Fe mineral, with the formula: $(Si_{11.888}Al_{0.112})(Mg_{7.313}Al_{0.154}Fe_{0.084})O_{30}(OH)_4(OH_2)_4{\cdot}x8H_2O$.

The fibres, arranged in the form of interwoven mats, are straight and have lengths varying between 2–6 μm and widths of 20–40 nm. Commonly, they are aggregated into units of two parallel-lying fibres, with a random orientation against each other, creating a dense network of pores. The high viscosity and external surface area (306–346 m^2g^{-1}) of the material, compared to those of the Spanish Vallecas sepiolite, suggest the high industrial suitability of this clay. The extent of the deposit is not known. Lithology and geomorphology indicate a lacustrine, closed basin evaporative environment of formation for this deposit. In contrast to the palaeolacustrine environments of formation of Spanish and Turkish sepiolite deposits, the El Bur sepiolite apparently is more recent.

The occurrence of Meerschaum (sepiolite) deposits in Somalia has been known for some time, and sporadically mentioned in reports (Ahrens, 1951; Grossher, 1978). Deposits of sepiolite in the El Bur area of Somalia were mentioned by Galán (1987) in his review of world reserves of this clay mineral. The Federal Statistical Office of Germany (1991) reported a yearly production of 10 t of sepiolite between the years 1985–1987, after 9 t in 1982. Recent political unrest thwarted plans for expansion of production and possible export. Production at present is for local consumption only.

Scientific studies of palygorskite, another fibrous clay mineral, are available from Northern Somalia where large amounts of palygorskite characterize soils of Quaternary age (Alaily *et al*., 1990). These soils occur on parent materials of different ages and with a varying lithology, under a semi-arid to arid climate. The provenance of this mineral is attributed to inheritance as well as to authigenic neoformation. Late Tertiary lagoonal sediments rich in palygorskite from Northern Somalia have been described by Hendriks *et al*. (1993). The origin of this mineral is, according to the authors, from reworking of older marine sediments, although minor pedogenic transformation of smectite to palygorskite may have occurred too. Studies by Boaler & Hodge (1964) indicated the presence of palygorskite in soils of Northern Somalia. These studies suggest that conditions for the formation and stability of palygorskite in Somalia are not unfavourable.

The first description of a Meerschaum (sepiolite) occurrence in the El Bur area of Central Somalia was by Stahr *et al*. (1990). They described a material extracted and worked by local inhabitants, that produced ceramic and popular art objects from the raw (unburned) clay. Access to the sites was, and still is, dangerous because of political unrest. Drechsel (1991) later described palygorskite and sepiolite occurrences in soils of the same area.

It is the objective of this paper to characterize the El Bur sepiolite chemically and mineralogically and to propose processes for its formation.

GEOLOGY AND GEOMORPHOLOGY

The major portion of the Somalia peninsula constitutes a wide sedimentation basin, into which a sequence of marine transgressions from the NE towards the SW have deposited huge sedimentary formations, beginning with the Jurassic and continuing into the Upper Tertiary. While Palaeozoic rocks apparently are absent, sandstone from the Triassic has been found only in Northern and Southern Somalia. Exposures of crystalline basement rocks are known only from the El Bur region in Central Somalia, and in Northern Somalia.

The El Bur area is situated in the Central Plateau that, with an area of 150,000 km^2, constitutes 1/4 of the surface of the Republic of Somalia (Fig. 1). This tableland is level to slightly undulating, and includes several sub-units (Fig. 2). The Lower Cretaceous Belet Uen limestone formation lies to the west, the 200–499 m thick upper Cretaceous to Eocene Jesomma sandstone more to the east and the Auradu fossil-rich limestone from the Lower Eocene. More to the east, the plateau is underlain by the Lower to Mid Eocene Taleh formation (up to

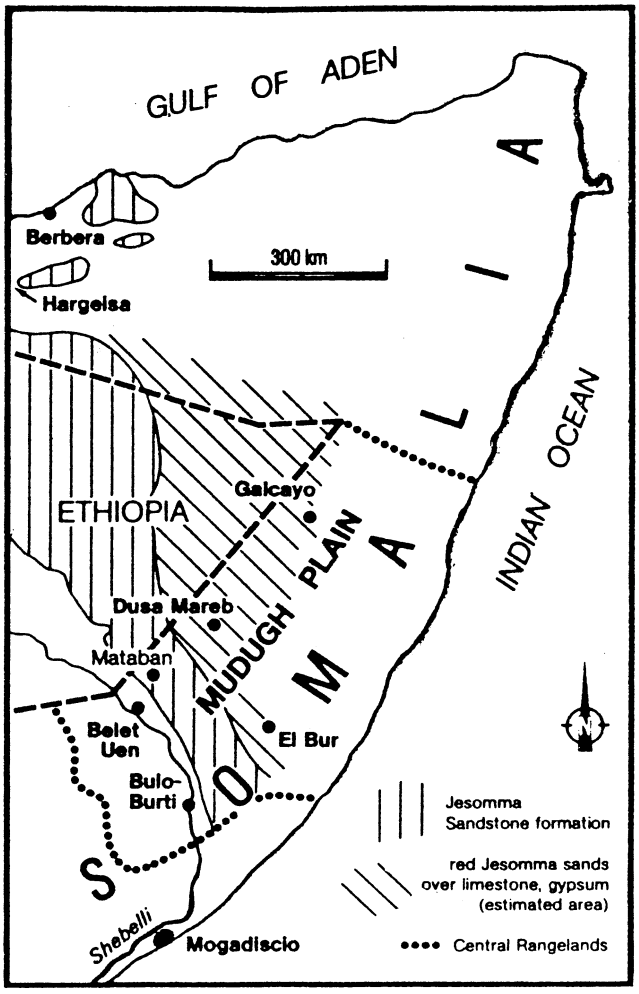

FIG. 1. El Bur location map in Central Somalia.

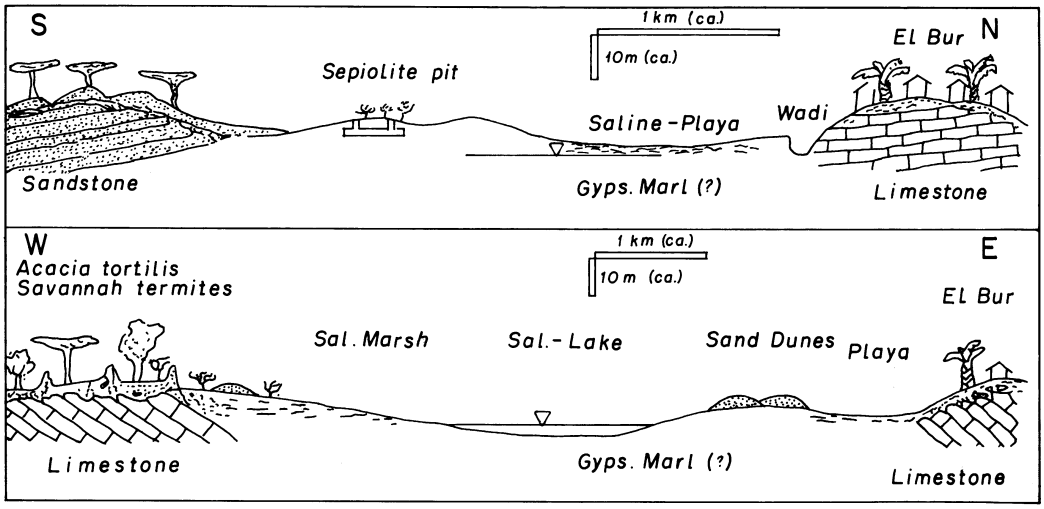

FIG. 2. Schematic cross-sections of El Bur sepiolite site, seen from east (upper) and from south (lower).

270 m thick) which includes limestone and various evaporites, with interlayering of marls and dolomites (Watson *et al*., 1982). Thus extensive gypsum deposits characterize this formation. Commonly, gypsum near the surface represents a hydration product of anhydrite. The Taleh formation is followed more to the north by nodular and massive, up to 400 m thick, limestones of the Middle to Upper Eocene Karkar formation. It is noteworthy that the landforms underlain by the Auradu, Taleh and Karkar formations are covered by a continuous layer, up to 3 m thick, of consolidated sands, with some occasional sand dunes. The sands, of a light yellow to reddish brown hue, are considered to be relatively old and, at present, resistant to wind erosion. Since they lie unconformably on the calcareous sediments, they are not considered to be their weathering products, and were probably blown in from the coastal sands or from the Jesomma sandstone formation to the west.

The depressions in this tableland have some playa-like characteristics, contain some gypsiferous marls and are dominated by evaporites, particularly gypsum, in a variety of forms, including selenite and transparent platy gypsum. The soils are moderately to highly saline and contain both palygorskite and sepiolite in their clay fraction (Drechsel, 1991). The climate of the area is semi-arid to arid with ~200 mm y^{-1} precipitation, falling in two short seasons. Somewhat more humid periods may have prevailed during the Pleistocene. The vegetation of this sparsely inhabited region consists of an Acacia tortilis savannah. Annual grasses provide some meagre pasture for the livestock of the partly nomadic population.

SITE DESCRIPTIONS

El Bur is situated ~350 km NNW from Mogadishu, on the Central Somalia Plateau, *ca*. 200 m above sea level. The area belongs to the 'southern gypsum' division of the Taleh formation (Watson *et al*., 1982).

To the west of the hamlet of El Bur, a slight depression contains a saline lake, fringed by a *ca*. 1 km wide saline playa (Fig. 2). The sepiolite deposits are situated south-east of the playa, about 3 km south of the hamlet, flanking the air-strip to Belo Burti.

The excavation pits used by local inhabitants are 2–3 m deep. Overburden consists of a saline Aridisol and lacustrine sedimentary deposits. Below a desert pavement is a dry, homogeneous, brown, loamy sand with few roots, to a depth of ~40 cm. Below that, at 40–100 cm depth, appears a dry, finely laminated, grey lacustrine sediment of hard consistency. Laminae are frequently fractured by gypsum or halite crystallite disintegration,

possibly as a result of dissolution. Between 100–170 cm this changes to a dry, massively-dense, white layer. At 160 cm, the lacustrine sediment is moist, yellowish-white, and again laminar. Below 200 cm, the white to yellowish, moist material is of a soft consistency, with occasional cracks. The massive layer has still some coarse pores with some remains of root-channels that are partly coated by Mn cutans. Gypsum crystallites can be discerned visually as well as gypsum pseudomorphs.

METHODS

Untreated crumbs of the material were examined by scanning electron microscopy (SEM), using a Jeol JXA 50A instrument with EDS attachment.

Untreated material was ground slightly and submitted to X-ray diffraction (XRD) by the powder method, using Cu-$K\alpha$ radiation on a Siemens 5000-D instrument. Washed material (to eliminate soluble salts) was examined by the combined differential thermal/gravimetric analysis method, using a Netzsch STA 409 EP instrument with a 10°/min heating rate. Sepiolite morphology was examined by electron microscopy, using a Zeiss Model EM10 transmission electron microscope (TEM) and a HRSEM ABT DS 150 F (Topcon Tokio) scanning electron microscope.

The chemical composition of untreated materials was obtained by X-ray fluorescence spectroscopy using a Siemens SRS 200 instrument. The viscosity of sepiolite suspensions was determined by the Ostwald method on a Cannon-Fenske viscosity-meter, produced by Schott. The BET surface area measurements were carried out in the Institute for Mineralogy, University of Tubingen, on a Gemini 2375 instrument after outgassing the samples in N_2 at 100°C for 1 h. Both of these determinations were also carried out on a Vallecas sepiolite sample for reference purposes. The density was determined by the displacement method using petrol, benzene or ethanol as immersion liquids.

The chemical composition of water extracts from the sepiolite deposit, obtained by equilibrating the material with water at a 1:1 ratio, was determined by conventional methods. Organic C was obtained by the difference between total C and carbonate C.

RESULTS

Chemistry

Table 1 indicates that Al, Ca, Na, K, Fe and Ti (expressed as oxides) are present only in very small amounts in all the layers examined. All layers except at 100–200 cm contain some impurities. Layers at 40–100 cm and 200–300 cm contain some halite, as was also confirmed by XRD (Table 3). Layers at 0–40 cm and 200–300 cm also contain calcite. The concentrations of calcite calculated from the CaO contents were 15.5 and

TABLE 1. Chemical composition (%) of fine earth (<2 mm) and clay (<2 μm) from a sepiolite excavation pit in El Bur, Central Somalia.

Layer (cm)	0–40		40–100		100–200		200–300	
	<2 mm	<2 μm	<2 mm	<2 μm	<2 mm	<2 μm	<2 mm	<2 μm
SiO_2	46.6	52.2	50.2	56.7	58.6	54.0	46.0	47.7
MgO	9.4	15.2	18.7	20.8	20.2	19.5	16.3	15.7
Al_2O_3	2.80	4.08	0.90	1.00	0.80	0.83	0.74	1.30
CaO	14.5	9.0	0.5	1.3	0.41	0.07	10.6	5.2
Na_2O	0.94	0.03	3.7	–	0.74	0.03	3.6	0.23
K_2O	1.04	1.10	0.46	0.47	0.54	0.40	0.42	0.63
TiO_2	0.30	0.40	0.11	0.12	0.11	0.10	0.09	0.18
Fe_2O_3	1.46	2.46	0.59	0.50	0.39	0.48	0.37	0.78
MnO	0.01	0.02	–	–	–	–	0.02	0.07
P_2O_5	0.02	0.03	–	0.04	–	0.02	–	0.05
ZrO	0.03	0.02	0.01	0.02	0.02	–	0.01	0.01
$H_2O(+)$	12.0	10.0	11.0	16.0	8.0	19.0	14.0	21.0
$H_2O(-)$	10.9	5.4	13.8	3.0	10.1	5.6	7.7	7.2

11.4% for the 0–40 cm and 200–300 cm layers, respectively. This was less than the carbonate calculated from the inorganic C contents (20.25 and 16.4% for the uppermost and lowermost layers, respectively), and suggests the presence of high-Mg calcite or even traces of dolomite. While carbonate is disseminated throughout the matrix of the layer at 0–40 cm, in the layer at 200–300 cm it appears as fissure coatings. This suggests that it represents reprecipitated carbonate from leaching out of the upper layer or derived from below (capillarity or surface discharge). In the clay fraction (<2 μm) separated from the bulk material, halite is absent and also the amount of carbonate is less (Table 1).

Using the Brauner-Preisinger model (Bailey, 1980) for ideal sepiolite:

$$Si_{12}Mg_8O_{30}(OH)_4(OH_2)_4{\cdot}8H_2O$$

the chemical composition of the clay (<2 μm) fractions of the second (40–100 cm) layer from the excavation pit was used for calculating the following formula for the El Bur sepiolite (assuming the presence of 5% quartz as impurity).

$$(Si_{11.888}\ Al_{0.112})(Mg_{7.313}\ Al_{0.154}\ Fe_{0.084})O_{30}\ (OH)_4(OH_2)_4{\cdot}8H_2O$$

This indicates a relatively small tetrahedral Al for Si substitution. Octahedral cation occupancy is low (7.551) and thus the extra positive charges created by Al substitution of Mg compensate only partly for the negative tetrahedral and octahedral charges. This explains the relatively high cation exchange capacity of the El Bur sepiolite, ranging between 240–360 mmol kg^{-1}. To be noted also is the very low Fe content of this sepiolite.

The pH of the sediment water extracts is moderately alkaline in the uppermost layer, mildly alkaline in the lower ones (Table 2). High concentrations of soluble salts are present in the second (40–100 cm) and fourth (200–300 cm) layers, as also shown by the XRD identification of halite in these layers. The dominant soluble cation is Na, followed by Mg, Ca and K (Table 2). The highest Mg/Ca ratio was found in the uppermost layer. Soluble K is relatively low. Among the anions, chlorides dominate, followed by sulphates.

XRD

Three out of the four layers examined consist of nearly pure sepiolite (Fig. 3). In the uppermost layer (0–40 cm) sepiolite is accompanied by some illite, distinguished by its 002 diffraction line from palygorskite. Calcite and minor amounts of quartz are present in this layer too. In the other layers (40–300 cm), quartz is present in trace to minor amounts (Table 3). In layers 40–100 cm and 200–300 cm, halite is present in trace amounts. Table 3 shows that in the three layers at 40–300 cm, all diffraction lines of sepiolite could be identified in powder diffractograms. The sharpness and intensity of the diffraction lines are comparable to those of the sepiolite from Vallecas, Spain, suggesting the high crystallinity of the material.

Ethylene glycol solvation did not result in any expansion of the 110 reflection in the 40–100 cm layer sepiolite. In the 200–300 cm layers, a slight expansion from 12.26 to 12.47 Å was observed, accompanied by contraction of the 130 spacing from 4.52 to 4.49 A.

Thermal analysis

The DTA analysis of the El Bur sepiolite (layers 40–100 cm) reveals four endothermic and one exothermic reactions (Fig. 4). The first endotherm,

TABLE 2. pH, $CaCO_3$ and soluble salts in the four layers of the El Bur excavation pit.

Horizon (cm)	pH (H_2O)	$CaCO_3$ %	C_{org} mg kg^{-1}	Water soluble salts Na^+	K^+	Mg^{2+} mmol kg^{-1}	Ca^{2+}	Cl^-	NO_3^-	SO_4^{2-}
0–40	8.59	20.2*	2.2	239	6.2	91.2	32.1	214	2.7	66
40–100	7.89	0	2.2	509	12.6	210	100.1	488	3.5	116
100–200	7.86	0	2.1	105	4.7	121	69.0	182	1.0	112
200–300	8.09	16.4*	2.0	526	11.6	201	87.8	674	5.0	116

*Calculated from inorganic carbon content

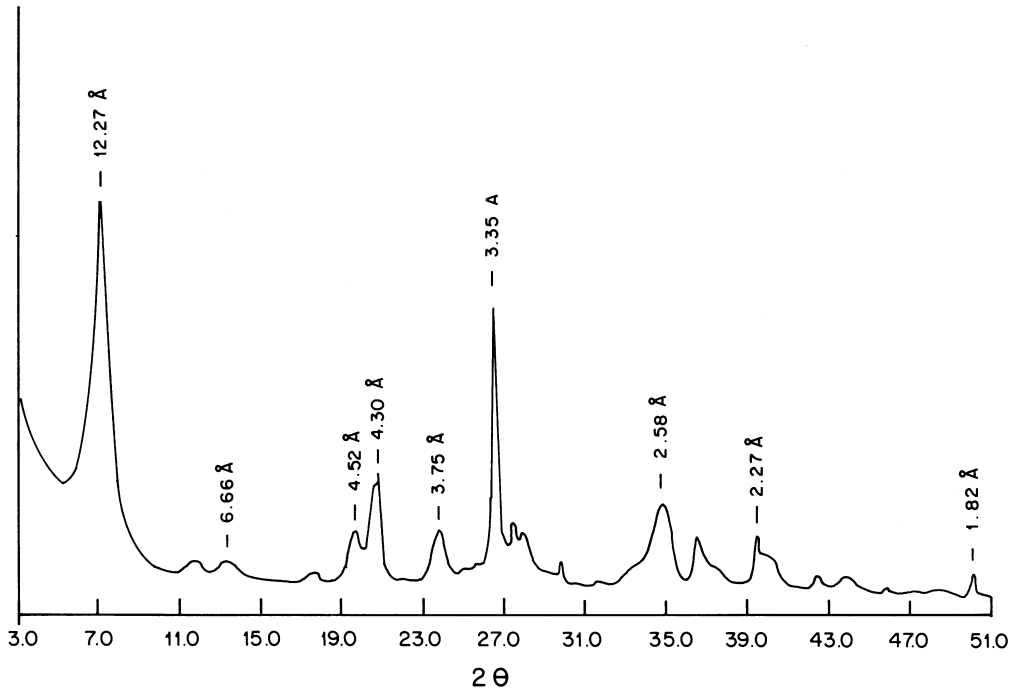

FIG. 3. Powder X-ray diffractogram (using Cu-$K\alpha$ radiation) of El Bur sepiolite from layer 40–100 cm. No impurities could be identified. The sepiolite diffraction line at 3.35 Å possibly overlays the major quartz line at 3.34 Å.

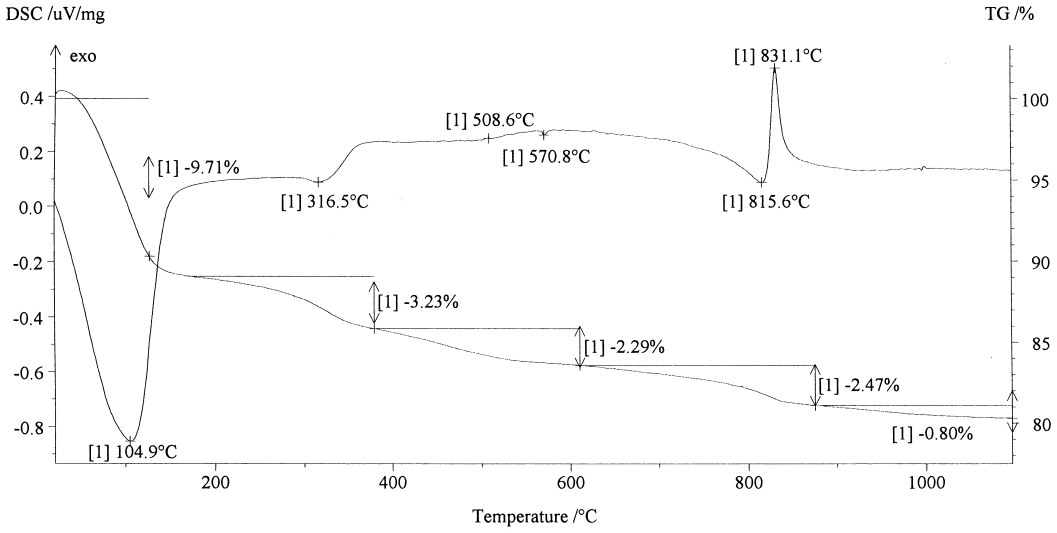

FIG. 4. Combined DTA and TGA tracings of El Bur sepiolite from layer 40–100 cm.

TABLE 3. X-ray powder data of different layers of the El Bur sepiolite compared to those of a sample from Vallecas, Spain.

Layer	40–100 cm		100–200 cm		200–300 cm		Vallecas	
	Å		Å		Å		Å	
hkl	d_{obs}	I/I_o	d_{obs}	I/I_o	d_{obs}	I/I_o	d_{obs}	I/I_o
110	12.27	100	12.29	57	12.32	100	12.19	100
130	7.58	13	7.58	8	7.59	13	7.51	10
040	6.66	14	6.66	8	6.67	12	6.67	10
150	5.03	10	5.03	7	5.04	9	5.03	8
031	4.52	21	4.52	12	4.52	18	4.50	17
131	4.30	32	4.29	30	4.31	26	4.31	24
221	–	–	3.98	6	–	–	3.98	7
260	3.75	21	3.74	12	3.74	18	3.75	19
241	3.54	12	–	–	–	–	3.53	10
080	3.35	76	3.48	100	3.35	73	3.34	26
331	3.20	20	3.25	24	3.24	28	3.19	17
	–	–	3.18	15	3.18	18	–	–
261	3.01	10	3.06	7	3.06	10	3.05	9
370	–	–	2.91	5	–	–	–	–
	2.83*	8	–	–	2.83*	27	2.82	6
460	2.68	12	2.70	7	2.68	11	2.67	10
	–		–		–		2.60	16
530	2.58	27	2.58	16	2.58	23	2.57	22
202	2.45	20	2.45	12	2.45	13	2.26	12
461	2.40	12	2.39	7	2.40	10	2.40	9
	2.28	18	2.28	13	2.26	13	2.26	12
312	2.25	15	–	–	–	–	–	–
640	2.13	11	2.13	10	2.13	10	2.12	6
402	2.06	10	2.06	6	2.06	8	2.06	8
	1.98*	7	1.98	8	1.99*	14	–	–
	–	–	1.92	11	–	–	1.94	4
	1.82		1.82	14	1.82	6	1.87	5
	1.54		1.54	15	1.54	17	1.55	6

* halite diffraction lines

between room temperature and 172.3°C, with the peak at 104.9°C, is associated with the elimination of adsorbed and zeolite H_2O. From the TGA curve it can be seen that the weight loss due to this reaction was 10.92%. The second endotherm, with a peak at 316.5°C, is due mainly to the loss of coordinated water. The weight loss between 170.4°C and 379.5°C associated with this reaction was 3.23%. The third broad endotherm, barely visible at 508.6°C, can be attributed to the elimination of the last part of the coordinated water and to the release of structural OH. Extending between 377.5°C and 610.5°C, 2.29% water was lost in this range. The marked endotherm at 815.6°C was followed immediately by a sharp and strong exotherm at 831.1°C. A weight loss of 2.47%, in the range between 610.5°C and 875.4°C may be related to the loss of the last portion of structural OH; 0.80% more weight loss was recorded between 875.4°C and 1096.5°C.

From Table 4, where the thermal reactions of the El Bur sepiolite are compared to those of the Vallecas sepiolite analysed under the same conditions, the similarity is remarkable. These losses are also similar to the theoretical ones given by Caillere *et al*. (1982), i.e. 11.1, 5.5 and 2.7% for the 20–260°C, 260–620°C and 620–1000°C intervals, respectively. The DTA curve exhibits the effects which, according to Peterson & Swaffield (1987), can be regarded as characteristic of sepiolite.

TABLE 4. Thermal reactions of the El Bur sepiolite (40–100 cm) compared to those of the sepiolite from Vallecas, Spain.

	El Bur, Somalia	Vallecas, Spain
Reaction temp. (°C)		
First endotherm	104.9	104.2
Second	316.5	311.8
Third	508.6	511.7
Fourth	815.6	823.3
Exotherm	831.1	834.9
Weight losses (%)		
RT–172.3	10.92	11.51
172.3–379.5	3.23	3.65
379.5–611.5	2.29	2.58
611.5–875.4	2.47	2.52
875.4–1096.6	0.80	0.69

Thermal characteristics of sepiolite from other layers are similar though not identical to those from 40–100 cm. In the 200–300 cm layer, the fourth endotherm is very small, and its peak temperature, as well as that of the exotherm, is lower.

IR analysis

The characteristic octahedral OH-stretching vibration is well formed, and appears in all spectra at 3693 cm^{-1} in the uppermost layer (0–40 cm), and at 3682 cm^{-1} in layer 100–200 cm (Fig. 5). Possibly, the spread in the frequencies of this band is related to the number of vacancies in the octahedral sites. Bands at 3620 cm^{-1}, 3564 cm^{-1} and 1625 cm^{-1} originate from channel water coordinated to Mg ions at the edges of the 2:1 ribbon layers. In the lowermost (200–300 cm) layer, the 1625 cm^{-1} band is very indistinct. The typical trioctahedral OH-deformation doublet bands at 696 and 641 cm^{-1} could also be observed in all samples. The position of the characteristic Si–O vibration band varied between 1218 cm^{-1} in the material from layer 200–300 cm to 1204 cm^{-1} in the layer 100–200 cm^{-1}. In the Vallecas sepiolite, this band appears at 1209 cm^{-1}.

Morphology

The morphology of single fibres was examined by TEM, and their structural arrangement by SEM.

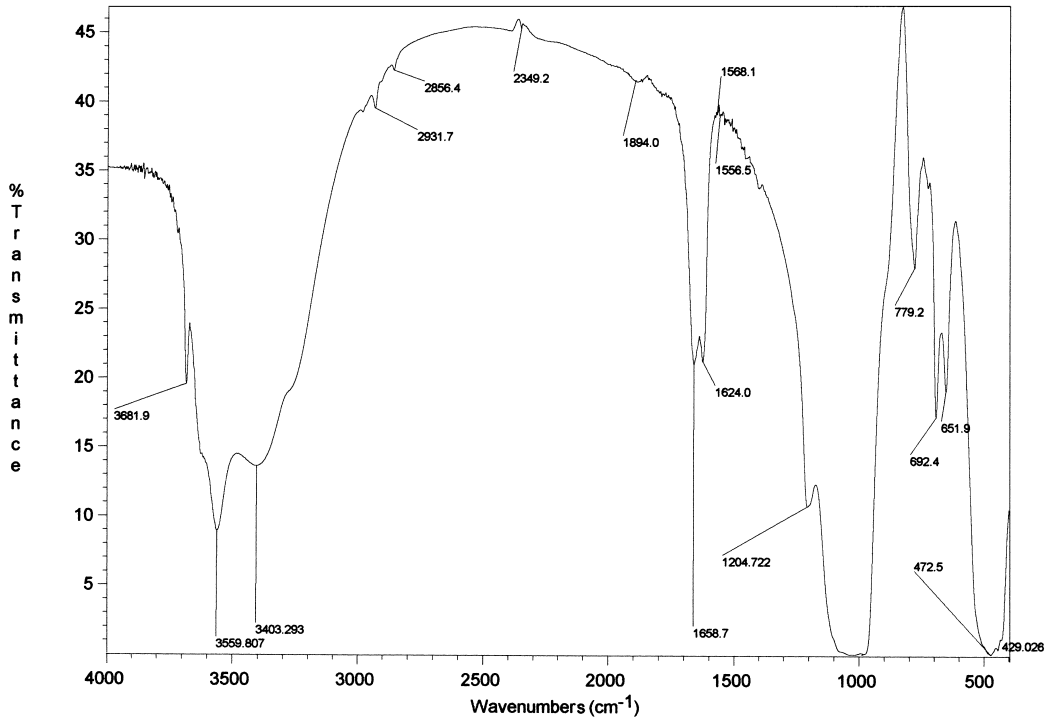

FIG. 5. IR spectrum of El Bur sepiolite from layer 100–200 cm.

The fibres have an approximate length of 1–2 μm in the uppermost layer, that increases to 2–4 μm in the lowermost layer (200–300 cm). The width of the fibres is 20–40 nm (Fig. 6). When dispersed, they are straight with no branching. In the lowermost layer (200–300 cm) features that could be interpreted as branching could sometimes be observed. In the uppermost layer, the fibres were accompanied by some small, plate-like crystallites, probably illite (as indicated by XRD).

The SEM observations revealed mats of interwoven, straight fibres. Commonly, the material was aggregated into units of two, sometimes more, parallel-lying and closely attached fibres, each with a width of 40–50 nm. These units appeared to have a random orientation against each other, creating a dense network of pores (Fig. 7). In the uppermost layer, these units were shorter, less straight, suggesting some disintegration.

The fibres are shorter than those observed for sepiolite formed by epigenetic weathering of mafic primary minerals nor were they arranged in thick strands aligned in a parallel pattern (Singer *et al*., 1992). Nor does the length of the fibres and their arrangement resemble that of the 'Meerschaum' sepiolite formed by magnesite replacement in Central Anatolia, Turkey (Yeniyol, 1995, Ece & Coban, 1994) where up to 20 μm length fibres, slightly to strongly curved and branching, and with parallel or subparallel orientation in bundles and mats or as coatings, pore-fillings and pore-bridging, were observed.

The morphology is also not similar to that described from the Madrid Basin (Spain) where the sepiolite has formed by the diagenetic alteration of smectite (Leguey *et al*., 1995). The idiomorphous morphology of the El Bur sepiolite fibres suggest crystal growth under conditions of supersaturation. Low supersaturation may give rise to long fibres coalesced into bundles (Gehring *et al*., 1995). The shorter fibres in a completely random orientation of the El Bur sepiolite are likely to have formed under higher supersaturation, associated with a stronger evaporative environment.

Surface area, viscosity, and bulk density

The largest external surface area, 346 m^2g^{-1}, was obtained in the 40–100 cm layer, the smallest, 306 m^2g^{-1}, in the uppermost (0–40 cm) layer (Table 5). The Vallecas sepiolite external surface, measured on the same instrument, was 224 m^2g^{-1}. This indicates a very high external surface area for the El Bur sepiolite.

At very low concentrations (1000 ppm), the viscosities are similar, and approximately equal to that of water. At higher suspension concentrations (1310 and 1740 ppm), the viscosity of the El Bur sepiolite, particularly that from layer 40–100 cm, is distinctly higher than that of the Vallecas sepiolite. The difference increases at higher concentrations.

The low bulk density of the El Bur sepiolite indicates the very high porosity of the material, also observed by SEM examination. The density is consistent to a depth of 200 cm, where it decreases sharply (Table 5).

DISCUSSION

Results indicate that, to a depth of 3 m at least, massive sepiolite is present in the surface sediments at El Bur. In the absence of detailed prospecting, the lateral extent of this deposit is not known. Lithological as well as geomorphological considerations suggest, however, that this, or similar surface deposits, might have a considerable extent. The vertical extent of this deposit is not known either. At depth of 3 m there were no indications for a transition to sediments of a different nature.

Data also indicate the relatively high purity of the deposit. Except for minor quantities of quartz and occasional carbonates and soluble salts, sepiolite clay is the sole component of all layers from 40 cm depth downward. Both external surface area and viscosity of this sepiolite are higher than that from Vallecas, and thus suggest the industrial suitability of this material.

Both the geology and geomorphology of the region indicate a lacustrine origin for the El Bur

TABLE 5. Bulk density, BET surface area and Ostwald viscosity (1740 ppm suspension) of the El Bur sepiolite compared to Vallecas sepiolite.

	Bulk density g cm^{-3}	Surface area m^2 g^{-1}	Viscosity mm^2/S*
El Bur			
0–40 cm	0.83	306	1.734
40–100 cm	0.76	346	3.211
100–200 cm	0.89	340	1.293
200–300 cm	0.49	342	n.d.
Vallecas	n.d.	224	1.171

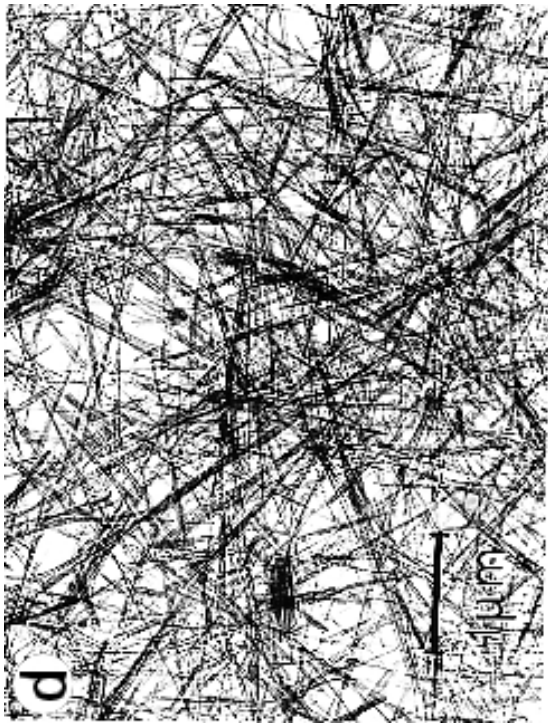

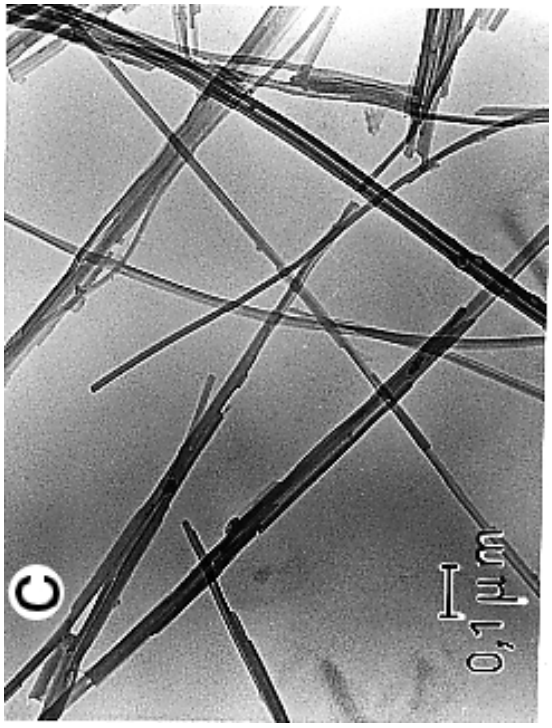

sepiolite. The physiography of the area is nearly level to slightly undulating, with shallow depressions that have playa-like characteristics and frequently contain saline lakes of a seasonal nature. Evaporites, particularly gypsum, are abundant in the surface sediments and occur in a variety of forms. Gypsiferous marls are common. The abundance of evaporites indicate a lacustrine, closed basin evaporative environment. These sediments are in accord with the present climate, which is semi-arid to arid and thus may have formed contemporaneously.

Millot (1964) in his studies of the Tertiary basins of north and west Africa, presented the classical scheme of clay mineral sequences in closed basin deposits. The species richest in Al and Fe are at the periphery and are succeeded basin-ward by more siliceous and Mg-rich clays, with sepiolite at the centre. Garrels & Mackenzie (1967) proposed direct precipitation of sepiolite from alkaline-saline lake water, concentrated by evaporative processes. In general terms, the sequence of more magnesian and siliceous clays basin-ward has been confirmed by subsequent studies, but apparently the formation of sepiolite as end-member is not ubiquitous (Jones & Galán, 1988). Crystalline rocks undergoing weathering, or volcanic ash, are commonly given as sources for Si, and Mg-rich carbonates, silicates or residual marine salts as those for Mg.

The geomorphological setting of the El Bur sepiolite is somewhat similar to that of the Tertiary lacustrine basins in Spain and in Turkey. The economically most significant of the Spanish deposits is from the Miocene Madrid basin (Galán & Castillo, 1984; Doval *et al*., 1986). In contrast with the Millot model, most sepiolite does not occur at the centre of the basin, but in marginal positions, crystalline rocks of bordering ranges being the major source for detritus and soluble Si. Fluctuating lacustrine brackish to saline waters are the principal contributors of Mg, probably derived from the recycling of Mesozoic marine evaporite strata.

The Turkish Eskisehir and Central Anatolian deposits are from the Miocene and had formed by the diagenetic replacement of magnesite pebbles with shallow burial under alkaline conditions in the vicinity of paleoshore lines (Ece & Coban, 1994; Yeniyol, 1995).

In contrast to these palaeolacustrine environments of formation, the El Bur sepiolite is Recent or Quaternary and appears to be forming at present. As such, this deposit could be likened to the occurrences described by Hay *et al*. (1995) in the Amboseli Basin, East Africa, the Amargosa Desert, Nevada (Hay *et al*., 1986), and to those described more recently by Webster & Jones (1994) from the southern High Plains, Texas.

In contrast to the Amargosa desert deposits, gypsum is a common associate of the El Bur sepiolite, suggesting that chemical precipitation had occurred from water with a higher salinity. The absence of other authigenic Mg clays, such as those described from the Amargosa desert, from the El Bur deposit, possibly indicates fewer fluctuations in the water chemistry in the latter.

The absence of any detrital clay minerals such as smectite or illite indicates that no significant overland run-off had taken place. The minor amounts of quartz may have been the result of some short-range aeolian input. The absence of detrital sheet minerals also supports the hypothesis that the sepiolite had formed by chemical precipitation and not by transformation of precursor minerals, such as palygorskite (Bachman & Machette, 1977). Webster & Jones (1994) deduced evaporatively induced salinity shifts from brackish to saline (perennial) or ephemeral-lake (playa) conditions from the predominance of sepiolite, interstratified Mg-smectite and palygorskite, respectively, in Pleistocene-Holocene lacustrine sediments in the southern High Plains, Texas.

No volcanic material or crystalline rocks are present in the immediate vicinity of the El Bur area that could have served as sources for the Si and Mg required for sepiolite precipitation. As an alternative source, sustained groundwater inflow could be considered. The presence of groundwater close to the surface in El Bur is indicated by the moist condition of the material that was sampled.

FIG. 6. Transmission electron micrographs of El Bur sepiolite (a) layer 0–40 cm; the length of the fibres is 1–2 μm; some small, plate-like crystallites probably represent illite. (b) and (c) layer 40–100 cm; length of the fibres is 2–4 μm; units of two or more, parallel-lying and closely attached fibres can be observed in (c); (d) layer 200–300 cm.

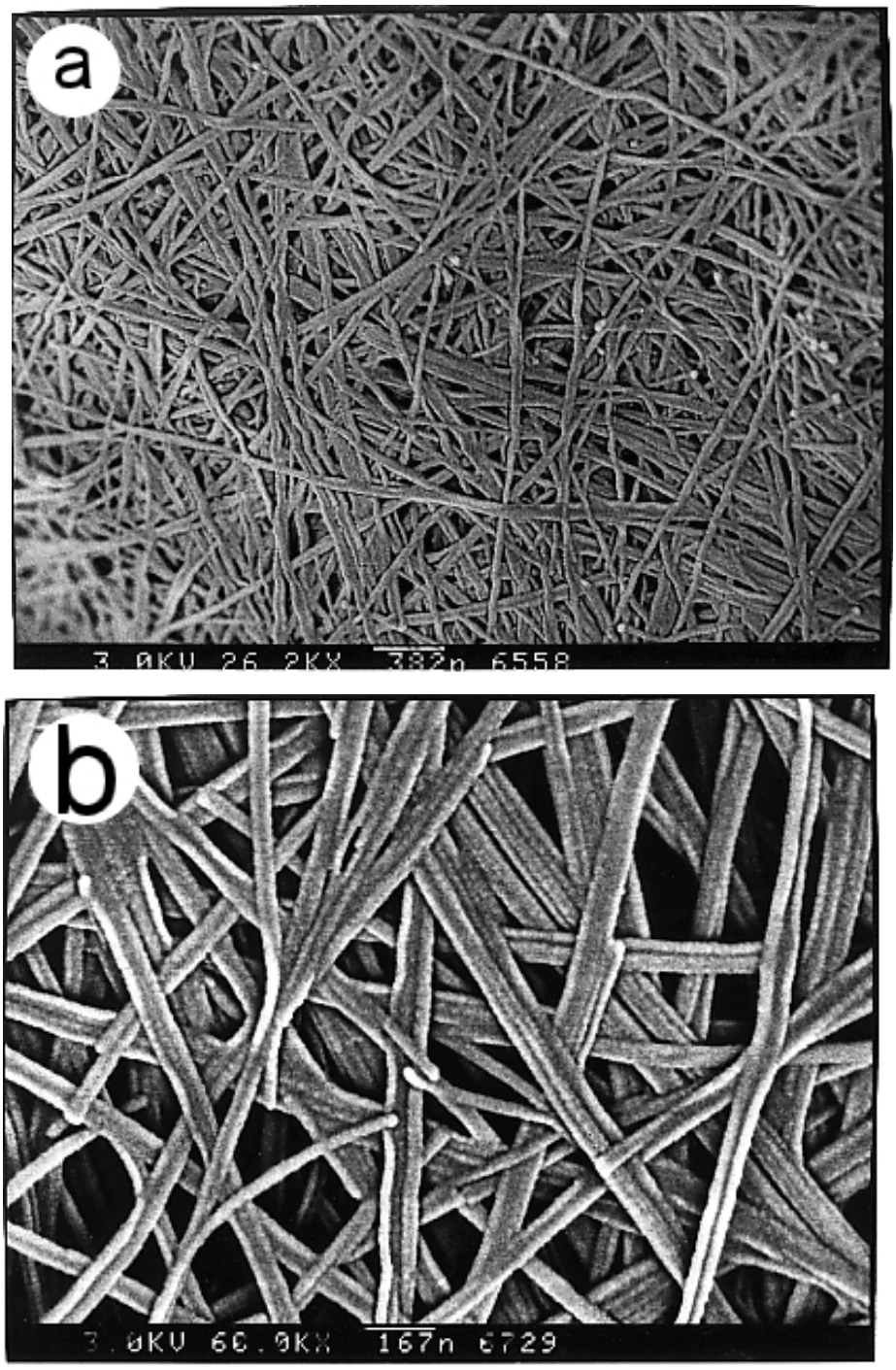

FIG. 7. Scanning electron micrographs of El Bur sepiolite from layer 200–300 cm (a) structure of mats formed by straight interwoven fibres; units of two, sometimes more, parallel-lying, closely attached fibres, can be observed in (b).

Sepiolitic clays at the margins of a pan in the Kalahari desert, SW Africa (Kautz & Porada, 1976) in the Amargosa desert, Nevada (Hay *et al*., 1986) and in the Amboseli basin, Kenya (Hay & Stoessell, 1984; Hay *et al*., 1995) are also proposed to have formed under the impact of Si/Mg-rich ground water. According to Hay *et al*. (1995), Si and Mg for Mg-rich clays in the Amboseli basin were supplied by lake- and ground-water. Different mixtures of dolomite, relatively Mg-rich ground-water with saline, alkaline lake water may have accounted for precipitation of sepiolite or other high-Mg clays at different times. The purity of the El Bur sepiolite supports the contention of Jones & Galán (1988) that the purest sepiolite deposits are the result of evaporative precipitation from dominantly groundwater-fed shallow water bodies lacking reactive clay detritus.

ACKNOWLEDGMENTS

The authors acknowledge the help of Mrs Harfold with the transmission electron microscopy, and that of Dr. Wurster with the scanning electron microscopy. Dr Baumann was extremely helpful in the viscosity measurements. Special thanks are also due to Prof. K. Nickel from Tubingen University for carrying out the surface area measurements. The opportunity to sample in the El Bur area was provided by the Special Research Program 308 of the German Research Foundation (DFG).

REFERENCES

Ahrens T.P. (1951) *A Reconnaissance Groundwater Survey of Somalia, East Africa*. Comitato interministriale per la reciostruzione, Roma.

Alaily F., Lassonczyk B., Huth A. & Genisor B. (1990) Genesis of soils in the arid part of north-east Somalia. *Berline Geowiss. Abh*. **(A) 120(2)**, 695–704. Berlin.

Bachman G.O. & Machette M.N. (1977) Calcic soils and calcretes in the southwestern United States. *U.S. Geol. Survey Open-File Rept*. **77–794**, 163 p.

Bailey S. (1980) Structures of clay minerals. Pp. 1–123 in: *Crystal Structures of Clay Minerals and their X-ray Identification* (G. Brindley & G. Brown, editors). Mineralogical Society, London.

Boaler S.B. & Hodge C.A. (1964) Observations on vegetation areas in the northern region, Somali Republic. *J. Ecol*., **52**, 511–544.

Caillere S., Henin S. & Rautureau M. (1983) *Mineralogie des Argiles*, Vol. 2, Masson, Paris.

Doval M., Calvo J.P., Brell J.M. & Jones B.F. (1986) Clay mineralogy of the Madrid basin: Comparison with other lacustrine closed basins. Pp. 188–189 in: *Geochemistry of the Earth Surface and Processes of Mineral Formation (abst.)* (R. Rodriguez-Climente & Y. Tardy, editors).

Drechsel P. (1991) Bodengesellschaften Centralsomalias: Ökologie und Genese. *Bayreuther Bodenkundliche Berichte*. **Band 19**, Bayreuth.

Ece O.I. & Coban F. (1994) Geology, occurrence and genesis of Eskisehir sepiolites, Turkey. *Clays Clay Miner*. **42**, 81–92.

Federal Statistical Office (1991) *Statistics of Foreign Countries, Somalia*. J. Be. Metzler and C. E. Poeschel Publ. Wiesbaden, Germany.

Galán E. (1987) Industrial applications of sepiolite from Vallecas-Vicalvaro, Spain: A review. *Proc. Int. Clay Conf. Denver*, 400–404.

Galán E. & Castillo A. (1984) Sepiolite-palygorskite in Spanish Tertiary Basins: Genetical patterns in continental environments. Pp. 87–124 in: *Palygorskite-Sepiolite, Occurrences, Genesis and Uses* (A. Singer & E. Galán, editors). Dev. Sedimentol. **37**. Elsevier, Amsterdam.

Garrels R.H. & MacKenzie F.T. (1967) Origin of the chemical composition of some springs and lakes. Pp. 222–242 in: *Equilibrium Concepts in Natural Water Systems* (W. Stumm, editor). American Chemical Society, Advances in Chemistry **v. 67**.

Gehring A.V., Keller P., Frey B. & Luster J. (1995) The occurrence of spherical morphology as evidence for changing conditions during the genesis of a sepiolite deposit. *Clay Miner*. **30**, 83–86.

Grossher D. (1978) *Somalia Hantiwadaag*. Kubler, Heidelberg.

Hay R.L. & Stoessell R.K. (1984) Sepiolite in the Amboseli Basin of Kenya: A new interpretation. Pp. 125–136 in: *Palygorskite-Sepiolite, Occurrences, Genesis and Uses* (A. Singer & E. Galán, editors). Dev. Sedimentol. **37**. Elsevier, Amsterdam.

Hay R.L., Pexton R.E., Teague T. & Kyser K. (1986) Spring-related carbonate rocks, Mg clays and associated minerals in Pliocene deposits of the Amargosa desert, Nevada and California. *Geol. Soc. Am. Bull*., **97**, 1488–1503.

Hay R.L., Hughes R.E., Kyser T.K., Glass H.D. & Lin J. (1995) Magnesium-rich clays of the Meerschaum mines in the Amboseli Basin, Tanzania and Kenya. *Clays Clay Miner*. **43**, 455–466.

Hendricks F., Behrens H., Busch W., Bussmann M., Gebhardt H., Gorler K., Reuleke D., Strouhal A. & Uhmann A. (1993) Detrital palygorskite in lacustrine and lagoonal clay-mineral associations of Late Tertiary age from Morocco and Somalia. *Zbl. Geol. Palaont. Teil 1, 1992 H. 5*, 415–436.

Jones B.F. & Galán E. (1988) Sepiolite and palygorskite. Pp. 631–674 in: *Hydrous Phyllosilicates* (S.W. Bailey, editor). Reviews in Mineralogy, Vol. **19**,

Mineralogical Society of America, Washington, D.C.
Kautz K. & Porada H. (1976) Sepiolite formation in a pan of the Kalahari. *N. Jb. Mineral Mh*. 545–559.
Leguey S., Martin-Rubi J., Casas J., Marta J., Cuevas J., Alvarez A. & Medina J. (1995) Diagenetic evolution and mineral fabric in sepiolitic materials from the Vicalvaro deposit (Madrid Basin). *Proc. 10th Int. Clay Conf. Adelaide*, 383–392.
Millot G. (1964) *Geologie des Argiles*, Masson and Cie, Paris, 510 pp.
Osman A.S., Farag H.A. & Abdi M.S. (1985) *Geology of Somalia*. Ministry of Minerals and Water Res., Mogadishu.
Peterson E. & Swaffield R. (1987) Thermal Analysis. Pp. 99–132 in: *A Handbook of Determinative Methods in Clay Mineralogy* (M.J. Wilson, editor), Blackie, Glasgow & London.
Singer A., Kirsten W.F.A. & Bühmann C. (1992) Occurrence of sepiolite in the northern Transvaal, South Africa. *S. Afr. J. Geol*. **95**, 165–170.
Stahr K., Zarei M. & Jahn R. (1990) Autigene Sepiolithbildung im Gebiet von El Bur (Zentral-Somalia). *Mitt. Dt. Bodenkund. Ges*. **62**, 147–150.
Watson R.M., Tippett C.F., Beckett J.J. & Scholes V. (1982) *Resource Management and Research*. Somali Democratic Republic, Central Rangelands Survey, Vol. 1 Parts 1 and 3, London (unpublished, copies in the Library of the NRA in Mogadishu).
Webster D.M. & Jones B.F. (1994) Paleoenvironmental implications of lacustrine clay minerals from the Double Lakes formation, southern High Plains, Texas. Pp. 159–172 in: *Sedimentology and Geochemistry of Modern and Ancient Saline Lakes*. SEPM Special Publ. No. **50**.
Yeniyol M. (1995) Meerschaum sepiolite and palygorskite ocurrence in Central Anatolia, Turkey. *Proc. 10th Int. Clay Conf. Adelaide*, 378–382.